Efficient generation of singlet oxygen by perylene diimide photosensitizers covalently bound to conjugate polymers

Agata Blacha-Grzechnik, Anna Drewniak, Krzysztof Z. Walczak,
Marek Szindler, Przemyslaw Ledwon

PII: S1010-6030(19)30972-4

DOI: https://doi.org/10.1016/j.jphotochem.2019.112161

Reference: JPC 112161

To appear in: *Journal of Photochemistry & Photobiology, A: Chemistry*

Received Date: 13 June 2019

Revised Date: 1 August 2019

Accepted Date: 11 October 2019

Please cite this article as: Blacha-Grzechnik A, Drewniak A, Z. Walczak K, Szindler M, Ledwon P, Efficient generation of singlet oxygen by perylene diimide photosensitizers covalently bound to conjugate polymers, *Journal of Photochemistry and amp; Photobiology, A: Chemistry* (2019), doi: https://doi.org/10.1016/j.jphotochem.2019.112161

Efficient generation of singlet oxygen by perylene diimide photosensitizers covalently bound to conjugate polymers

Agata Blacha-Grzechnik[a], Anna Drewniak[b], Krzysztof Z. Walczak[b], Marek Szindler[c], Przemyslaw Ledwon*[a]

[a] Silesian University of Technology, Department of Physical Chemistry and Technology of Polymers, Strzody 9, 44-100 Gliwice, Poland

[b] Silesian University of Technology, Department of Organic Chemistry, Bioorganic Chemistry and Biotechnology, Krzywoustego 4, 44-100 Gliwice, Poland.

[c] Silesian University of Technology, Institute of Engineering Materials and Biomaterials, Konarskiego 18A, 44-100 Gliwice, Poland

*Corresponding author; email: przemyslaw.ledwon@polsl.pl; tel.: +48322371305; postal adress: Strzody 9, 44-100 Gliwice, Poland

Graphical abstract

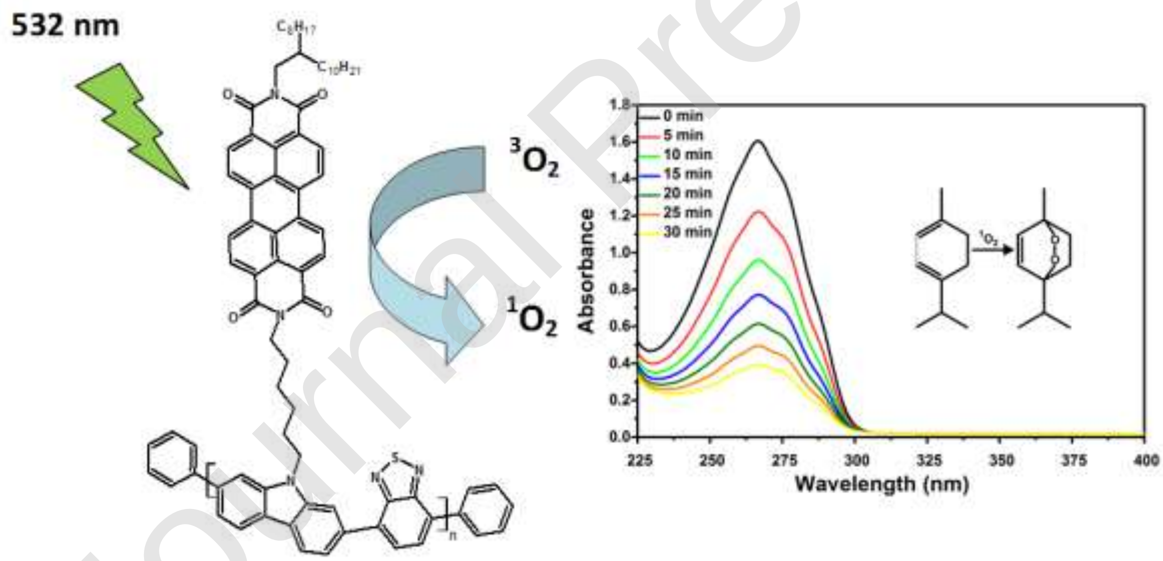

Highlights

- The photoactive polymer films were formed by spin-coating on glass substrates.
- The deposited layers were active under the green light illumination
- The immobilized perylene diimide (PDI) units retain activity towards ^{1}O2 generation
- The layers were applied in α-terpinene photooxidation

Abstract

New conjugated polymers with perylene diimides (PDI) as pendant groups were synthesized and deposited on glass substrates by the spin coating. The resulting thin films were characterized by UV-Vis, Raman spectroscopy and profilometry. It was shown that PDI photosensitizers retain its photoactivity after covalent immobilization and the formed layers can be applied as efficient and environmentally stable source of singlet oxygen, $^1O_2$, as tested with 1,3-diphenylisobenzofuna (DPBF) specific trap. Additionally, the α-terpinene heterogeneous photooxidation was studied as the practical use of singlet oxygen generated by this novel PDI-based materials. The use of such heterogeneous source of singlet oxygen can be beneficial for in the fine chemicals' synthesis, due to simplified products' isolation and purification step.

Keywords

singlet oxygen, perylene diimide, photochemistry, α-terpinene photooxidation, photosensitizer, conjugated polymers

1. Introduction

Singlet oxygen $^1O_2$ has been under high research interest for over 50 years as a possible candidate for application in Photodynamic Therapy (PDT), fine chemicals' synthesis or wastewater treatment [1–4]. This excited state of oxygen without unpaired electrons is formed in the photosensitization process, where photosensitizer molecule is excited by light illumination and transfers its energy to $^3O_2$ molecules [5–7]. Various types of compounds able to generate singlet oxygen are known: dyes, aromatic hydrocarbons, porphyrins, phthalocyanines, conjugated polymers, transition metals complexes, semiconductors oxides, carbon-based nanostructures and described lately - perylene diimide (PDI) derivatives [5,8–10]. The latter could be particularly interesting due to high quantum yields of singlet oxygen photogeneration [11], high photostability [12] and broad ability to modified its structure [13]. Singlet oxygen has higher reactivity and electrophilicity, but also lower stability and shorter lifetime than triplet oxygen, so it has to be generated *in situ* into reaction mixture. High attention is nowadays paid on developing methods of photoactive molecules' deposition on solid support, in order to form heterogenous photocatalysts applicable in fine chemicals' synthesis or wastewater treatment. Though, typically lower yields of $^1O_2$ photogeneration are observed for immobilized photosensitizers, such approach possess several advantages over homogenous photocatalysis, like ease of operation or easier product separation and purification [5,14–17]. Our group has recently shown that thin organic films of phenothiazines formed in the process of electrochemical polymerization or electrochemical reduction of the diazonium salts, are able to generate active singlet oxygen in the reaction mixture, leading to the oxidation of 1,3-diphenylisobenzofuran (DPBF), phenol or α-terpinene [18–21].

Carbazoles are one of the most common compounds used as building blocks of conjugated polymers [22–24]. The great interest in carbazole derivatives results from the low cost of the starting material, easy modification of its structure, and its good stability. In this work carbazole was chosen as building-block for synthesis of monomer consisting of dibromocarbazole derivative with PDI side unit linked by hexyl groups. Three photoactive materials were synthesized: pCB-PDI and pCC-PDI consisting of conjugated main polymeric chain and pendant PDI units linked by hexyl groups, and unmodified pCB (Scheme 1). Conjugated pCB polymer is known as a donor-acceptor polymer with absorption of visible light, unlike poly(2,7-carbazole) films, that are almost transparent and do not absorb visible radiation [25,26]. Moreover, the chosen polymeric backbone and covalently attached photosensitizer, are both highly stable in air and in various organic solvents [27,28], which makes them attractive candidates for the heterogeneous generation of singlet oxygen in industrially important oxidation reactions [5].

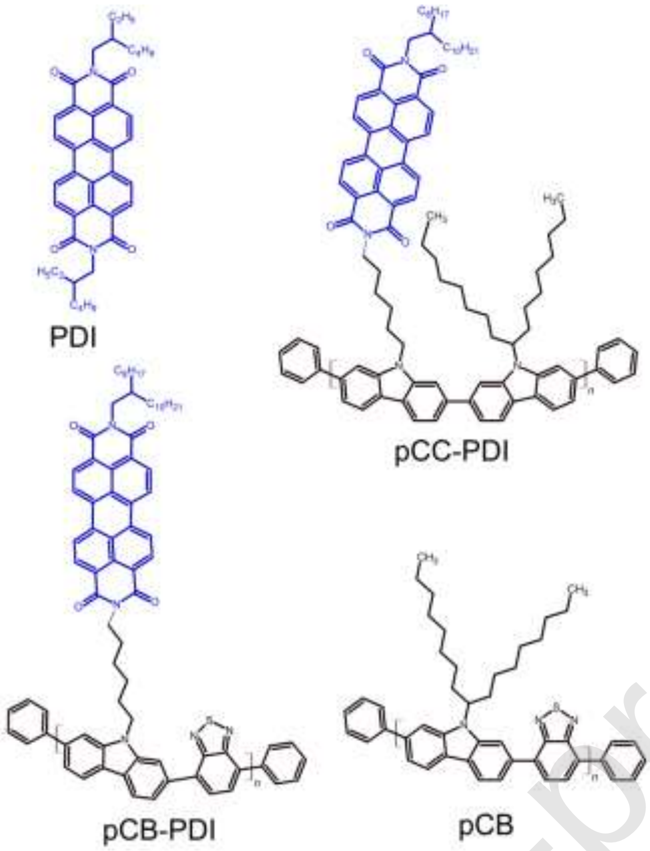

Scheme 1 The structures of the presented compounds

2. Materials and methods

2.1 General information

All chemicals and solvents were purchased from Sigma Aldrich, TCI or ChemPure unless otherwise stated. Given yields refer to isolated compounds unless otherwise stated. Synthesis procedure includes synthesis of monomer *N*-(2-n-octyldodecyl)-*N'*-[6-(2,7-dibromo-*9H*-carbazol-9-yl)hexyl]perylene-3,4,9,10-tetracarboxylic diimide (**4**) and synthesis of pCC-PDI, pCB-PDI and pCB macromolecules. Other monomers were purchased commercially and used without purification: 2,1,3-Benzothiadiazole-4,7-diboronic acid bis(pinacol) ester (>98%) and 9-(1-Octylnonyl)-2,7-bis(4,4,5,5-tetramethyl-1,3,2-dioxaborolan-2-yl)-9*H*-carbazole (>97%) were purchased from Osilla. 2,7-Dibromo-9-(9-heptadecyl)carbazole (>98%) were purchased from TCI. Purification step by a column chromatography was done on silica gel packed column (70-230 mesh, 63-200 µm, 60Å). ^{1}H NMR and ^{13}C NMR were recorded on Varian Mercury Plus 600 (600 MHz) or Varian Unity Inova (300 MHz) spectrometers, the chemical shifts are given in ppm using TMS as an internal standard. The mass spectra were recorded with AB Sciex 4000 QTRAP (HRMS) or

Shimadzu Biotech Axima Performance (MALDI-TOF MS) mass spectrometers. 1,3-diphenylisobenzofuran (DPBF) (Acros Organics, purity >97%) in methanol (Acros Organics, 99.9%) was used as a specific $^1O_2$ quencher. α-Terpinene (TCI, purity 90%) in acetonitrile (Sigma Aldrich, HPLC grade) was employed as a substrate in the photooxidation reaction.

2.2 Formation and characterization of photoactive films

pCB-PDI, pCB and pCC-PDI layers were deposited on 1 cm x 1 cm borosilicate glass slides (PGO) by spin coating (2000 rpm) from polymer solutions (6,6 $mg \cdot cm^{-3}$) in chlorobenzene with temperature of 70 ^{0}C. The thickness of the polymer films were estimated by the Profilm3D profilometer.

UV-Vis spectra of the deposited films were collected in quartz cuvette (Hellma Analytics, 2 mm) using of Hewlett Packard 8452A UV-Vis spectrometer. Raman spectra were collected by means of Renishaw inVia Raman Microsope (Renishaw, Inc., New Mills, UK) equipped with diode excitation laser with the wavelength of 514 nm, 2400-lines grating and 50x objective. All Raman spectra were subjected to smoothing and baseline subtraction procedures using Renishaw software.

The 2D and 3D topographic 2×2µm images were performed with XE-100 Park Systems atomic force microscope (AFM). The microscope was set to non-contact mode. The RMS and Ra coefficient values were determined with XEI software. RMS was defined as rough mean square parameter and Ra was defined as the arithmetic mean deviation of the profile from the mean line.

2.3. Procedure of singlet oxygen photogeneration

Singlet oxygen photogeneration was investigated using 0.05 mM solution of 1,3-diphenylisobenzofuran (DPBF) in methanol [29]. DPBF is known as specific singlet oxygen quencher [30], reacting *via* 1,3-addition mechanism with $^1O_2$ of singlet oxygen [1]**.** The progress of the reaction, *i.e.* the drop in the absorbance of DPBF at 410 nm, was monitored by means of Hewlett Packard 8452A UV-Vis spectrometer. The quartz cuvette (Hellma Analytics, 10 mm x 4 mm) applied in the measurements was arranged as a thin layer cell possessing a cavity of 10 mm path length and thickness of 2 mm. This cavity was created between the cuvette wall and the freshly prepared photoactive layer deposited on glass. 532 nm diode laser (Oxxius, LCX-532L-150-CSB-PPA model, 150 mW maximum power reduced to 50 mW) was employed as an excitation light source illuminating ca. 0.5 cm^2 of sample's surface.

The singlet oxygen quantum yields for each PDI-containing layers were calculated using Equation 1 and Rose Bengal as the reference (??$_{RB}$ = 0.80 in methanol[31]).

$$\boldsymbol{\Phi_i = \Phi_{RB} \cdot \frac{m_i}{m_{RB}} \cdot \frac{\alpha_{RB}}{\alpha_i}} \text{ (Equation 1),}$$

where the indexes *i* and *RB* indicate investigated PDI-polymer structure and Rose Bengal, respectively, Φ is the quantum yield of singlet oxygen photogeneration; m is the slope of a trend line of change in the absorbance of DPBF (at 410 nm) vs. time and α is the absorption correction factor given by $\alpha = 1 - 10^{-A}$ (A is the absorbance at 532 nm)[32–34].

2.4 Procedure of α-terpinene photooxidation

PCB-PDI/glass layer was then applied as a source of singlet oxygen in the oxidation of α-terpinene in acetonitrile, resulting in the formation of ascaridole[35]. The progress of the reaction was monitored similarly as in the case of DPBF. The yield of photooxidation reaction, thus the singlet oxygen generation, was determined based on the decrease in the absorption of α-terpinene at 266 nm. The initial concentration of α-terpinene was 0.25 mM. The concentration of α-terpinene at the given time was found applying Lambert-Beer's law for the absorption maximum at 266 nm ($\varepsilon_{terpinene}$ = 6.95 mM^{-1}cm^{-1} in acetonitrile). In order to investigate possible re-use of the photoactive layer, the process was repeated 5 times.

3. Results and Discussion

3.1 Synthesis

Investigated photoactive materials were synthesized using Suzuki type coupling using appropriate monomers (Scheme 2) [36].

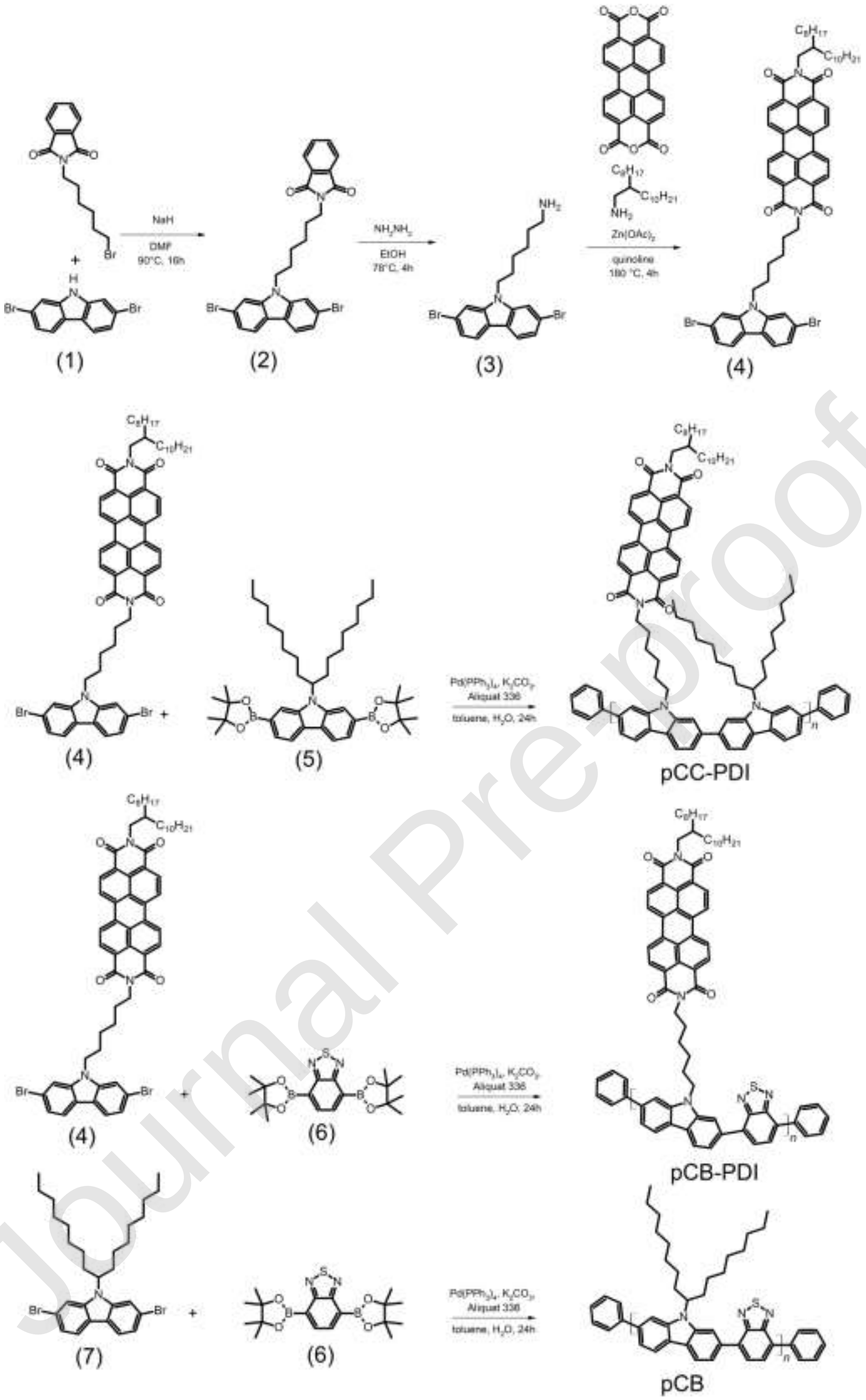

Scheme 2 Synthesis of studied polymers

N-[6-(2,7-dibromo-9*H*-carbazol-9-yl)hexyl]phthalimide) **2** was obtained from 2,7-dibromo-9*H*-carbazole and *N*-(6-bromohexyl)phthalimide. Compound **2** was treated with the hydrazine monohydrate in an ethanol to obtain 6-(2,7-dibromo-9*H*-carbazol-9-yl)hexyl-1-amine **3**. Compound **3** was acquired as a mixture of phthalhydrazide in an approximate ratio of 1:1 (the ^{1}H and ^{13}C NMR spectrum of the precipitate is shown in Figure S3 and S4). The presence of phthalhydrazide did not interfere with diimide **4** synthesis.

The synthesis of **4** was conducted in one-step reaction of condensation by reacting equimolar ratio of the amine **3,** 2-n-octyldodecylamine and 3,4,9,10-perylenetetracarboxylic dianhydride in quinoline. Monomer **4** was purified by a column chromatography and precipitated with methanol. Polymers **pCC-PDI**, **pCB-PDI** and **pCB** were synthesized by Suzuki coupling polymerization using $Pd(PPh_3)_4$ as catalyst. Polymers were obtained with high yields and purified by Soxhlet apparatus.

^{1}H NMR spectra of pCC-PDI and pCB-PDI show broad signals in the range 8.63-7.30 and 8.64-7.28 respectively. Such feature is characteristic for NMR spectra of polymers containing PDI units and results from PDI aggregation occurring at the solutions' concentration used for NMR spectra recording [37–42]. In the range 7.29-7.12 in pCC-PDI spectrum, signals from the end groups are clearly visible.

MALDI-TOF measurements show that pCB-PDI is oligomeric/polymeric material with rather low molecular mass up to 4.2 kDa, while pCC-PDI and pCB are polymers with molecular mass up to 8.3 kDa and 9.3 kDa, respectively.

3.2 Spectroscopic and AFM characterization of the photoactive layers

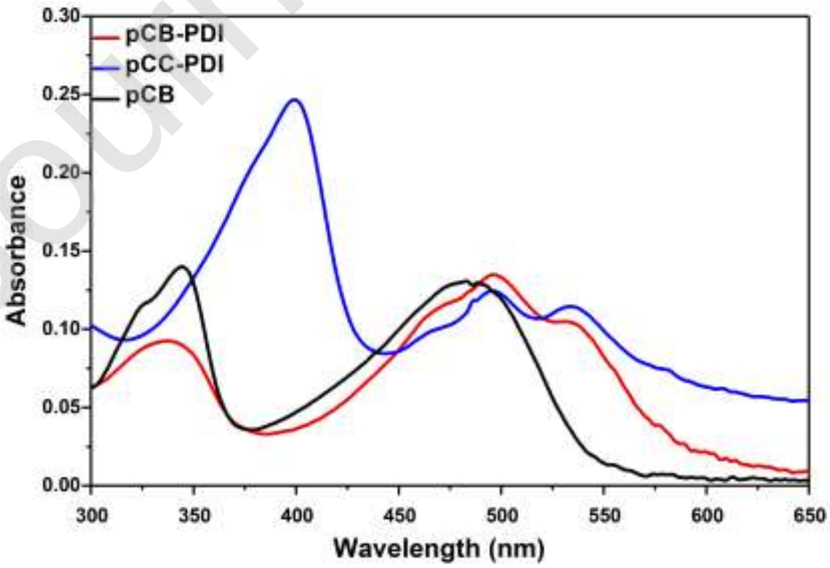

Figure 1. UV-Vis spectra of pCB-PDI, pCC-PDI and pCB deposited on borosilicate glass

The synthesized polymers were deposited on borosilicate glass by spin-coating to form films having a thickness of 280 nm, 190 nm and 220 nm for pCB-PDI, pCB and pCC-PDI respectively. Figure 1 presents UV-Vis spectra of formed polymeric layers. In the case of pCB-PDI and pCC-PDI films, absorption bands characteristic for PDI unit are observed at ca. 500 and 545 nm [43,44]. Those bands are partially overlapping in pCB-PDI spectrum with pCB absorption having maximum at ca. 475 nm. For pCC-PDI absorption coming from conjugate polymer chain is blue-shifted to 400 nm and thus separated from PDI absorption bands. Based on these results, 532 nm laser was selected as an illumination source for singlet oxygen photogeneration. Such wavelength should cause excitation of PDI units in both pCB-PDI and pCC-PDI layers, and by pCB polymeric backbone.

The structure of the formed thin films was in turn investigated by means of Raman spectroscopy. Figure 2 presents Raman spectra recorded for deposited pCB-PDI, pCC-PDI and pCB layers. In the case of the first two layers, the vibrations characteristic for PDI unit are observed at ca. 1300 cm^{-1} and 1380 cm^{-1} corresponding to C-H bending and at ca. 1570/1588 cm^{-1} arising from C-C/C=C stretching in perylene core [45,46]. Those vibrations are absent for the unmodified pCB layer. For the polymeric films bearing benzothiadiazole groups, *i.e.* pCB and pCB-PDI, signals at ca. 1270 cm^{-1} and 1345 cm^{-1} coming from C-C stretching in benzothiadiazole aromatic ring and C=N stretching + C=N-S deformation, respectively, are observed [47]. For all deposited layers characteristic vibrations for carbazole units (eg. 1626 cm^{-1}, ν (C=C)) and benzene rings (eg. 1458 cm^{-1}, δ (C-H)) are present [48–50], confirming expected structure of the investigated films.

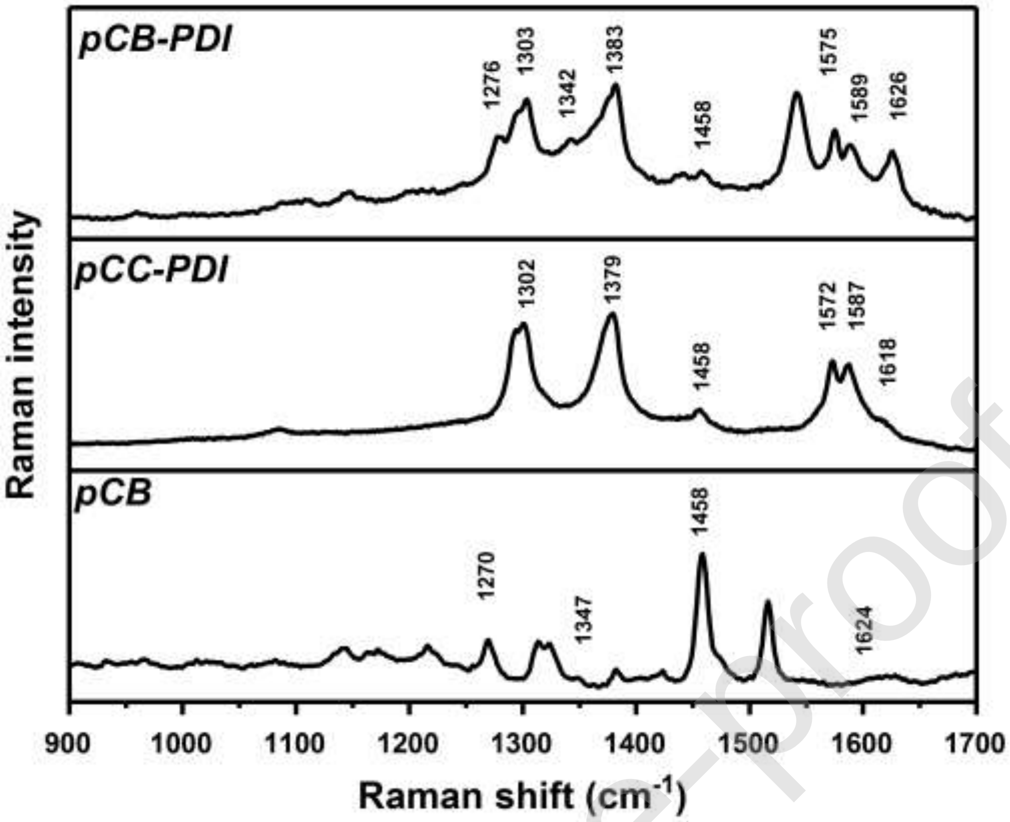

Figure 2. Raman spectra of pCB-PDI, pCC-PDI and pCB films deposited on borosilicate glass

The 2D and 3D topographic images of photoactive polymer thin films are shown in Figures.3a–f. The histograms of irregularities are compared in Figures S15a-c (please see Supporting information). The values of RMS and Ra coefficients are included in Table 1. The deposited layers are continuous and uniform. No impurities, precipitates, or delamination have been registered. It has been found out in the images, that repetitive aggregations of atoms have a similar geometrical features. The presence of PDI unit in the layer resulted in a slight increase in roughness. The RMS and R_a parameters were respectively: for the pCB-PDI 1.23 and 0.97 nm, for pCC-PDI 0.46 and 0.36 nm while for pure PCB are 0.34 and 0.25 nm. The histograms obtained with AFM microscope software present the number of pixels with different height depending on its value, that corresponds to the area occupied with the highest and lowest points. The obtained histograms are in good coincidence with parameters in Table 1.

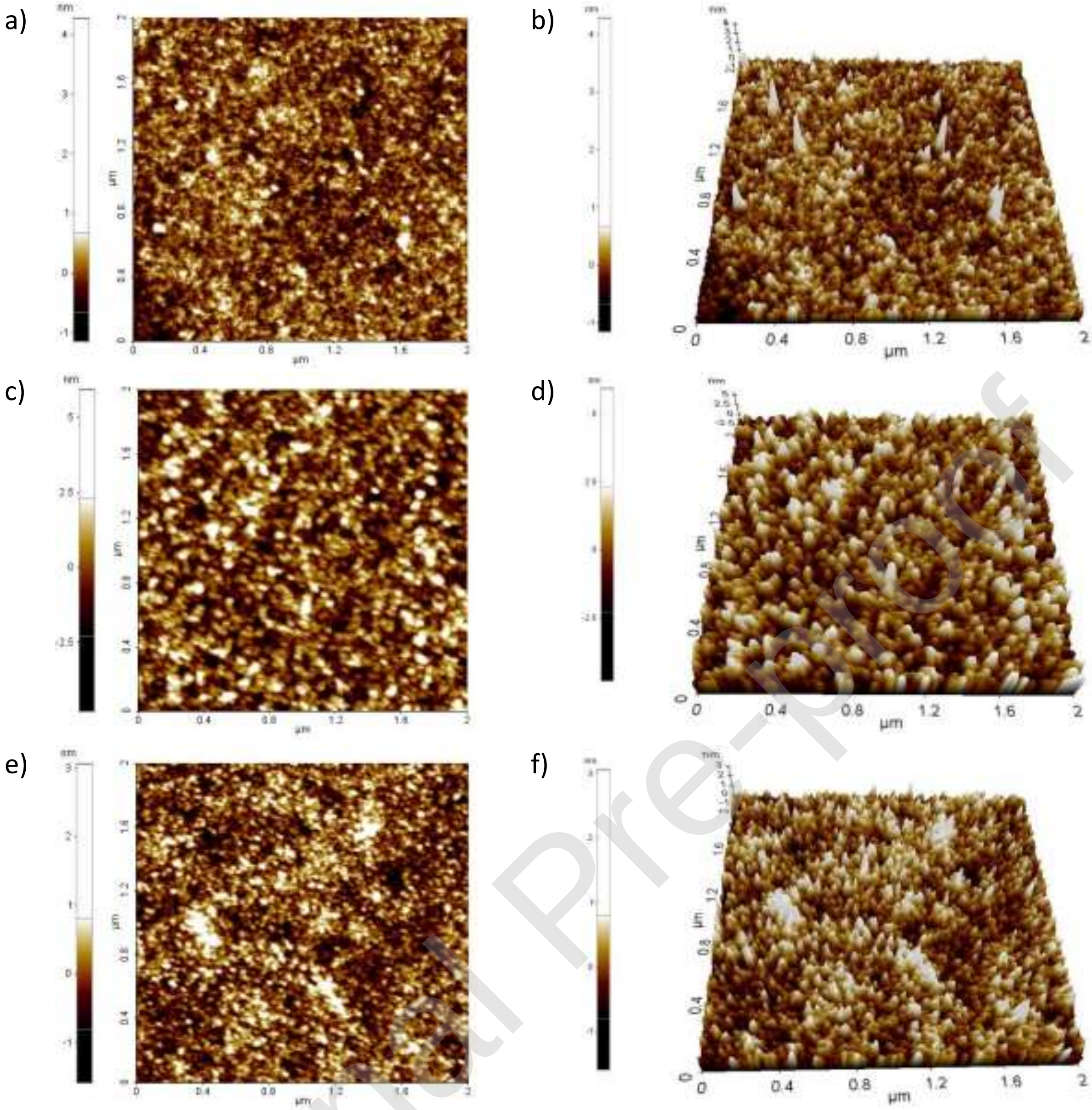

Figure 3. AFM 2D and 3D images of the Surface topography of: pCB (a,b); pCB-pdi (c,d); pCC-PDI (e,f)

Table 1 Summary of roughness parameters for deposited photoactive polymer thin films

Sample	Surface area $[\mu m^2]$	RMS [nm]	R_a [nm]	max. irregularity [nm]
PCB	4.00	0.34	0.25	4.28
pCB-PDI	4.00	1.23	0.97	5.92
pCC-PDI	4.00	0.46	0.36	3.06

3.3 Singlet oxygen photogeneration measurements

Various specific singlet oxygen chemical traps can be applied in the indirect detection of this ROS form [30,51]. In this work, the most commonly used 1,3-diphenylisobenzofuran (DPBF) was used as a specific $^1O_2$ quencher [1]. Figure 4 presents the example of set of UV-Vis spectra of DPBF solution in methanol recorded during illumination of pCB-PDI layer with 532 nm laser with power of 50 mW. The clear decrease in the DPBF's absorption at 410 nm can be observed indicating its reaction with singlet oxygen photogenerated by pCB-PDI photoactive film [52]. Importantly, the investigated layer is stable under applied conditions, since no new band at ca. 500 nm is appearing during process. Similar results were obtained when pCC-PDI layer was illuminated, which confirms that in both cases PDI photosensitizer retains its photoactivity after covalent bonding to the conjugate polymer support. Additionally, since also weak drop in DPBF absorption was observed for pCB polymer itself, it may be suspected that during pCB-PDI illumination the combined $^1O_2$ photogeneration by PDI photosensitizer and conjugated backbone occurs.

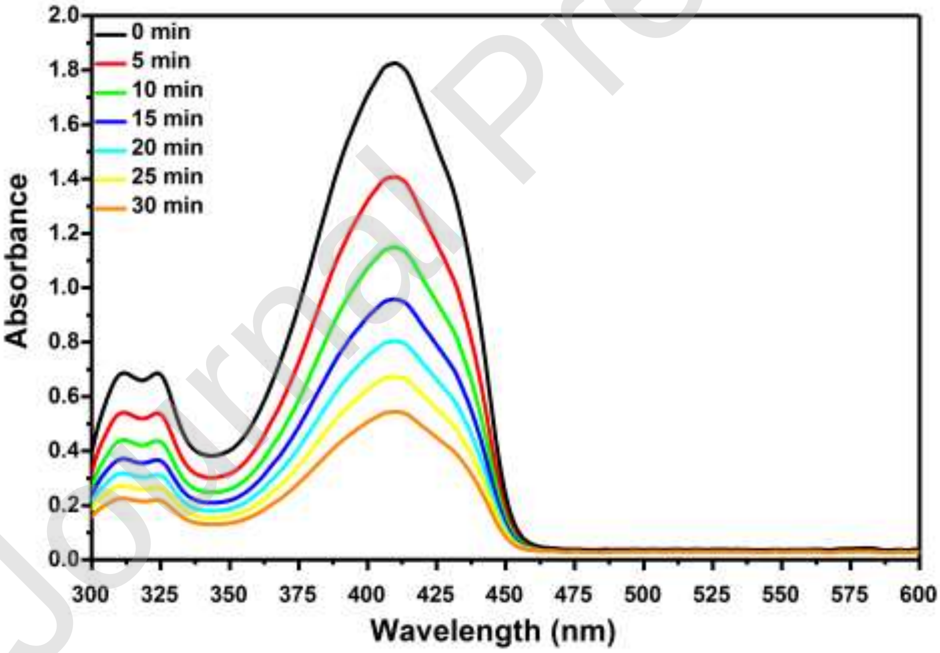

Figure 4. UV-Vis spectra of DPBF recorded during illumination of pCB-PDI/glass layer with 532 nm laser

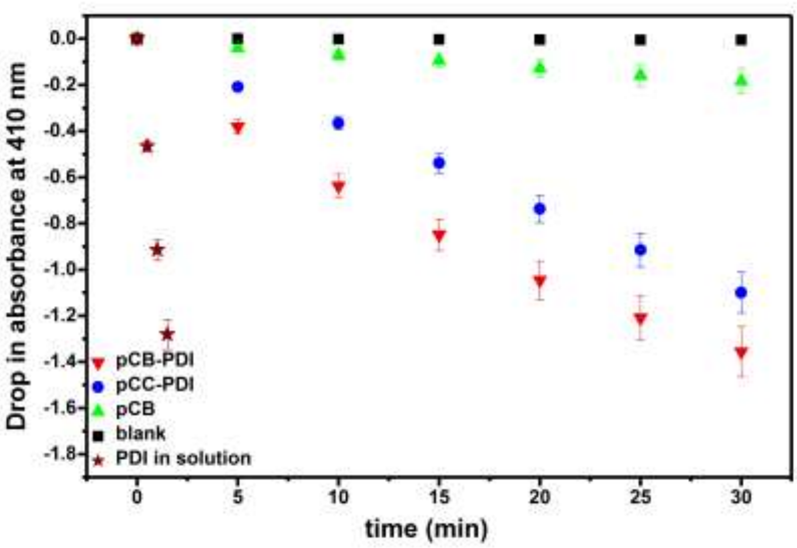

Figure 5. Drop in the absorption of DPBF at 410 nm during illumination of PDI, pCB-PDI/glass, pCC-PDI/glass, pCB/glass and bare borosilicate glass

Table 2. Quantum yield of singlet oxygen photogeneration calculated with respect to Rose Bengal as a standard

Photosensitizer	**??**
PDI in solution	0.36 ± 0.04
pCB-PDI	0.09 ± 0.01
pCC-PDI	0.06 ± 0.01

The comparison of the effectiveness of DPBF's oxidation, i.e. $^1O_2$ photogeneration, by all deposited layers is presented in Figure 5 and Table 2. As it can be seen, the highest yield of investigated photoprocess was observed for pCB-PDI film, in which both PDI and polymeric chain are activated by green radiation. Under applied conditions, pCC-PDI layer, in which only PDI photosensitizer is being excited shows slightly lower effectiveness, while singlet oxygen production by pCB polymer itself is rather poor. Autooxidation of DPBF is excluded, since almost no drop in DPBF's absorption is observed when unmodified borosilicate glass slide is illuminated with green laser (Figure 5)[53]. As expected, the quantum yield of singlet oxygen photogeneration by deposited photoactive layers is several times lower than for PDI photosensitizer present in the solution phase, as presented in the Table 2. However, as mentioned, the heterogeneous approach in photocatalysis is more favorable for industrial applications ensuring easier product purification and separation, and re-use of catalyst. Importantly, as tested by UV-Vis and Raman spectroscopy, the deposited layers were stable under applied process conditions and the pendant PDI group was not detached from the polymeric backbone and released to the reaction mixture.

3.4 Oxidation of α-terpinene

In the next step, pCB-PDI photoactive layer, showing the highest efficiency in the singlet oxygen photogeneration, has been tested as a source of singlet oxygen in the photooxidation of α-terpinene. This industrially important process results in the formation of ascaridole – the commonly used anthelmintic drug. In this work, the process was conducted in acetonitrile with 532 nm laser as an excitation source. The progress of the reaction was monitored by UV-Vis spectroscopy as the decrease in α-terpinene absorption at 266 nm [35].

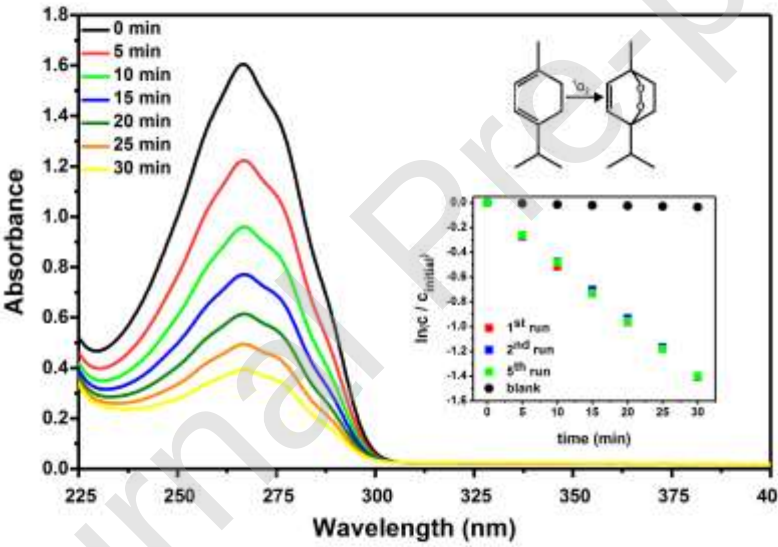

Figure 6. UV-Vis spectra of α-terpinene recorded during illumination of pCB-PDI/glass layer with 532 nm laser; inset: drop in concentration of α-terpinene during illumination of pCB-PDI/glass in the 1st, 2nd and 5th use glass and bare borosilicate glass

Figure 6 shows UV-Vis spectra of α-terpinene recorded in the course of illumination of pCB-PDI layer. The clear decrease in α-terpinene absorption at 266 nm is observed, due to its reaction with $^1O_2$ [17,54]. Since almost no drop in the absorption of α-terpinene is observed during illumination of bare borosilicate glass (Figure 6 inset), the self-degradation of substrate is excluded. Similarly to methanol environment the pCB-PDI layer is not being destructed nor dissolved in the reaction medium, i.e. acetonitrile, during the process.

The rate constant of the photooxidation of α-terpinene was determined based on the decrease in its concentration in time. The plot of $\ln(c_{terpinene}/c_{terpinene,initial})$ as a function of time gives the straight line, which indicates pseudo first-order reaction under applied conditions [55]. It was also found that only small drop in the effectiveness was observed when the pCB-PDI layer was re-used: ca. 6% decrease in the photoreaction yield for 5th use of tested material (Figure 6 inset), which indicates that the deposited layer maintains its high photoactivity after usage and can be re-used in the consecutive processes.

Note, that since the synthesized polymers are soluble in chloroform and/or chlorobenzene, they can be easily deposited on solid substrates, like glass by e.g. spin coating technique. On the other hand, due to their insolubility and high stability of such in such solvents as acetonitrile or methanol, they can be applied as the effective source of singlet oxygen in heterogeneous synthesis of fine chemicals. The results obtained for pCB-PDI indicate that this type of materials consisting with conjugated polymers and PDI moieties can be used as complementary sensitizers in the photooxidation processes. It can be expected that such systems may find application in the photooxidation processes including light sources with broader irradiation wwavelength range, for example white light sources. The use of common source of light and the use of solid sensitizers is considered beneficial for industrial processes from a practical point of view and strongly agrees with *green chemistry* concepts.

4. Conclusions

In summary, different conjugated polymers with pendant PDI groups deposited on the glass support were investigated as a source of singlet oxygen in methanol and acetonitrile under green light illumination. PDI-based polymer films show high efficiency in $^1O_2$ photogeneration tested by the reaction with DPBF specific trap. The presented results show that such materials can be effectively applied in the form of thin photoactive films in the commercially important process of α-terpinene oxidation without introduction of additional reagents into the reaction mixture, which is extremely beneficial for the isolation and purification of reaction products. Moreover, the green light irradiation is beneficial compared to higher energy irradiation often used in generation of singlet oxygen, due to smaller possibility of side reactions occurring along with the reducing of irradiation energy.

Notes

The authors declare no competing financial interest.

Acknowledgements

The work was financed by National Science Centre, Poland under grants no. 2015/17/D/ST5/01343 and 2016/21/D/ST5/01641. We acknowledge Karol Knop for contributing to synthetic work.

References

(1) DeRosa, M. C.; Crutchley, R. J. Photosensitized Singlet Oxygen and Its Applications. *Coord. Chem. Rev.* **2002**, *233-234*, 351–371. https://doi.org/10.1016/S0010-8545(02)00034-6.

(2) Nonell, S.; Flors, C. *Singlet Oxygen: Applications in Biosciences and Nanosciences*; Nonell, S., Flors, C., Eds.; Royal Society of Chemistry, 2016. https://doi.org/10.1039/9781782622208.

(3) Zhang, X.-F. BODIPY Photosensitizers Based on PET and Heavy Atom Effect: A Comparative Study on the Efficient Formation of Excited Triplet State and Singlet Oxygen in BODIPY Dimers and Monomers. *J. Photochem. Photobiol. A Chem.* **2018**, *355*, 431–443. https://doi.org/10.1016/j.jphotochem.2017.07.019.

(4) Westberg, M.; Bregnhøj, M.; Blázquez-Castro, A.; Breitenbach, T.; Etzerodt, M.; Ogilby, P. R. Control of Singlet Oxygen Production in Experiments Performed on Single Mammalian Cells. *J. Photochem. Photobiol. A Chem.* **2016**, *321*, 297–308. https://doi.org/10.1016/j.jphotochem.2016.01.028.

(5) Wahlen, J.; Vos, D. E. De; Jacobs, P. A.; Alsters, L. Solid Materials as Sources for Synthetically Useful Singlet Oxygen. *Adv. Synth. Catal.* **2004**, *346*, 152–164. https://doi.org/10.1002/adsc.200303224.

(6) Tanaka, F.; Tsumura, K.; Furuta, T.; Iwamoto, K.; Okamoto, M. Efficiencies of Singlet Oxygen Production and Rate Constants for Oxygen Quenching in the S 1 State of Dicyanonaphthalenes and Related Compounds. *Photochem. Photobiol. Sci.* **2008**, *7* (1), 56–62. https://doi.org/10.1039/B711781G.

(7) Krasnovsky Jr., A. A. Singlet Molecular Oxygen: Early History of Spectroscopic and Photochemical Studies with Contributions of A.N. Terenin and Terenin's School. *J. Photochem. Photobiol. A Chem.* **2018**, *354*, 11–24. https://doi.org/10.1016/j.jphotochem.2017.07.013.

(8) Stasheuski, A. S.; Galievsky, V. A.; Stupak, A. P.; Dzhagarov, B. M.; Jin, M.; Chung,

B. H.; Jeong, J. Y. Photophysical Properties and Singlet Oxygen Generation Efficiencies of Water-Soluble Fullerene Nanoparticles. *Photochem. Photobiol.* **2014**, *90*, 997–1003. https://doi.org/10.1111/php.12294.

(9) Zou, H.; Jin, F.; Song, X.; Xing, J. Singlet Oxygen Generation of Photosensitizers Effectively Activated by Nd3+-Doped Upconversion Nanoparticles of Luminescence Intensity Enhancing with Shell Thickness Decreasing. *Appl. Surf. Sci.* **2017**, *400*, 81–89. https://doi.org/10.1016/j.apsusc.2016.12.174.

(10) Yukruk, F.; Dogan, A. L.; Canpinar, H.; Guc, D.; Akkaya, E. U. Water-Soluble Green Perylenediimide (PDI) Dyes as Potential Sensitizers for Photodynamic Therapy. **2005**, No. 6, 2004–2006. https://doi.org/10.1021/ol050841g.

(11) Dinçalp, H.; Kızılok, Ş.; İçli, S. Targeted Singlet Oxygen Generation Using Different DNA-Interacting Perylene Diimide Type Photosensitizers. *J. Fluoresc.* **2014**, *24* (3), 917–924. https://doi.org/10.1007/s10895-014-1372-5.

(12) Wu, Y.; Zhen, Y.; Ma, Y.; Zheng, R.; Wang, Z.; Fu, H. Exceptional Intersystem Crossing in Di(perylene Bisimide)s: A Structural Platform toward Photosensitizers for Singlet Oxygen Generation. *J. Phys. Chem. Lett.* **2010**, *1* (17), 2499–2502. https://doi.org/10.1021/jz1008328.

(13) Huang, C.; Barlow, S.; Marder, S. R. Perylene-3,4,9,10-Tetracarboxylic Acid Diimides: Synthesis, Physical Properties, and Use in Organic Electronics. *J. Org. Chem.* **2011**, *76* (8), 2386–2407. https://doi.org/10.1021/jo2001963.

(14) Sautrot-Ba, P.; Malval, J.; Weiss-maurin, M.; Paul, J.; Blacha-Grzechnik, A.; Tomane, S.; Mazeran, P.-E.; Lalevee, J.; Langlois, V.; Versace, D.-L. Paprika, Gallic Acid, and Visible Light: The Green Combination for the Synthesis of Biocide Coatings. *ACS Sustain. Chem. Eng.* **2018**, *6*, 104–109. https://doi.org/10.1021/acssuschemeng.7b03723.

(15) Gryglik, D.; Miller, J. S.; Ledakowicz, S. Solar Energy Utilization in Degradation of 2-Chlorophenol by Immobilized Photosensitizers. *Sol. Energy* **2004**, *77* (5), 615–623. https://doi.org/10.1016/j.solener.2004.03.029.

(16) Ribeiro, S. M.; Serra, A. C.; Rocha Gonsalves, A. M. d. A. Covalently Immobilized Porphyrins as Photooxidation Catalysts. *Tetrahedron* **2007**, *63* (33), 7885–7891. https://doi.org/10.1016/j.tet.2007.05.084.

(17) Kyriakopoulos, J.; Tzirakis, M. D.; Panagiotou, G. D.; Alberti, M. N.; Triantafyllidis, K. S.; Giannakaki, S.; Bourikas, K.; Kordulis, C.; Orfanopoulos, M.; Lycourghiotis, A. Highly Active Catalysts for the Photooxidation of Organic Compounds by Deposition

of [60] Fullerene onto the MCM-41 Surface : A Green Approach for the Synthesis of Fine Chemicals. "*Applied Catal. B, Environ.* **2012**, *117-118*, 36–48. https://doi.org/10.1016/j.apcatb.2011.12.024.

(18) Blacha-Grzechnik, A.; Piwowar, K.; Krukiewicz, K.; Koscielniak, P.; Szuber, J.; Zak, J. K. Photogeneration of Singlet Oxygen by the Phenothiazine Derivatives Covalently Bound to the Surface-Modified Glassy Carbon. *Appl. Surf. Sci.* **2016**, *371*, 151–159.

(19) Piwowar, K.; Blacha-Grzechnik, A.; Bernas, P.; Zak, J. Phenol Degradation in Heterogeneous System Generating Singlet Oxygen Employing Light Activated Electropolymerized Phenothiazines. *Appl. Surf. Sci.* **2015**, *359*, 426–431.

(20) Blacha-Grzechnik, A.; Piwowar, K.; Koscielniak, P.; Kwoka, M.; Szuber, J.; Zak, J. Phenothiazines Grafted on the Electrode Surface from Diazonium Salt. *Electrochim. Acta* **2015**, *182*, 1085–1092. https://doi.org/10.1016/j.electacta.2015.10.017.

(21) Blacha-Grzechnik, A.; Piwowar, K.; Zdyb, T.; Krzywiecki, M. Formation of poly(Azure A) -C60 Photoactive Layer as a Novel Approach in the Heterogeneous Photogeneration of Singlet Oxygen. *Appl. Surf. Sci.* **2018**, *457* (April), 221–228. https://doi.org/10.1016/j.apsusc.2018.06.262.

(22) Sathiyan, G.; Sivakumar, E. K. T.; Ganesamoorthy, R.; Thangamuthu, R.; Sakthivel, P. Review of Carbazole Based Conjugated Molecules for Highly Efficient Organic Solar Cell Application. *Tetrahedron Lett.* **2016**, *57* (3), 243–252. https://doi.org/10.1016/j.tetlet.2015.12.057.

(23) Higginbotham, H.; Karon, K.; Ledwon, P.; Data, P. Carbazoles in Optoelectronic Applications. *Disp. Imaging* **2017**, *2*, 207–216.

(24) Grazulevicius, J. V.; Strohriegl, P.; Pielichowski, J.; Pielichowski, K. Carbazole-Containing Polymers: Synthesis, Properties and Applications. *Prog. Polym. Sci.* **2003**, *28* (9), 1297–1353. https://doi.org/10.1016/S0079-6700(03)00036-4.

(25) Yasutani, Y.; Honsho, Y.; Saeki, A.; Seki, S. Polycarbazoles: Relationship between Intra- and Intermolecular Charge Carrier Transports. *Synth. Met.* **2012**, *162* (17-18), 1713–1721. https://doi.org/10.1016/j.synthmet.2012.07.005.

(26) Iraqi, A.; Wataru, I. Preparation and Properties of 2,7-Linked N -Alkyl-9 H -Carbazole Main-Chain Polymers. *Chem. Mater.* **2004**, *16* (3), 442–448. https://doi.org/10.1021/cm031078s.

(27) Ma, L.; Guo, Y.; Wen, Y.; Liu, Y.; Zhan, X. High-Mobility, Air Stable Bottom-Contact N-Channel Thin Film Transistors Based on N,N ′-Ditridecyl Perylene Diimide. *Appl. Phys. Lett.* **2013**, *103* (20), 203303. https://doi.org/10.1063/1.4831971.

(28) Wang, Y.; Michinobu, T. Benzothiadiazole and Its π-Extended, Heteroannulated Derivatives: Useful Acceptor Building Blocks for High-Performance Donor–acceptor Polymers in Organic Electronics. *J. Mater. Chem. C* **2016**, *4* (26), 6200–6214. https://doi.org/10.1039/C6TC01860B.

(29) Wainwright, M. Phenothiazinium Photosensitisers: V. Photobactericidal Activities of Chromophore-Methylated Phenothiazinium Salts. *Dye. Pigment.* **2007**, *73* (1), 7–12. https://doi.org/10.1016/j.dyepig.2005.10.001.

(30) Wainwright, M.; Meegan, K.; Loughran, C.; Giddens, R. M. Phenothiazinium Photosensitisers, Part VI: Photobactericidal Asymmetric Derivatives. *Dye. Pigment.* **2009**, *82* (3), 387–391. https://doi.org/10.1016/j.dyepig.2009.02.011.

(31) Lv, F.; Yu, Y.; Hao, E.; Yu, C.; Wang, H.; Jiao, L. Highly Regioselective α -Formylation and α -Acylation of BODIPY Dyes via Tandem Cross-Dehydrogenative Coupling with in Situ Deprotection. *Org. Biomol. Chem.* **2019**, No. 20, 1–44.

(32) Lambert, C. R.; Kochevar, I. E. Does Rose Bengal Triplet Generate Superoxide Anion？ *J. Am. Chem. Soc.* **1996**, No. 11, 3297–3298. https://doi.org/10.1021/ja9600800.

(33) Burguete, M. I.; Galindo, F.; Gavara, R.; Luis, S. V; Moreno, M.; Russell, D. A. Singlet Oxygen Generation Using a Porous Monolithic Polymer Supported Photosensitizer : Potential Application to the Photodynamic Destruction of Melanoma Cells. *Photochem. Photobiol. Sci.* **2009**, *8*, 37–44. https://doi.org/10.1039/b810921d.

(34) Epelde-Elezcano, N.; Martinez-Martinez, V.; Pena-Cabrera, E.; Gomez-Duran, C. F. A.; Arbelo, I. L.; Lacombe, S. Modulation of Singlet Oxygen Generation in Halogenated BODIPY Dyes by Substitution at Their Meso Position : Towards a Solvent-Independent Standard in the Vis Region. *RSC Adv.* **2016**, No. 6, 41991–41998. https://doi.org/10.1039/c6ra05820e.

(35) Ronzani, F.; Costarramone, N.; Blanc, S.; Benabbou, A. K.; Bechec, M. Le; Pigot, T.; Oelgemöller, M.; Lacombe, S. Visible-Light Photosensitized Oxidation of α-Terpinene Using Novel Silica-Supported Sensitizers: Photooxygenation vs. Photodehydrogenation. *J. Catal.* **2013**, *303*, 164–174. https://doi.org/10.1016/j.jcat.2013.04.001.

(36) Drewniak, A.; Tomczyk, M.; Hanusek, L.; Mielanczyk, A.; Walczak, K.; Nitschke, P.; Hajduk, B.; Ledwon, P. The Effect of Aromatic Diimide Side Groups on the π-Conjugated Polymer Properties. *Polymers (Basel).* **2018**, *10* (5), 487. https://doi.org/10.3390/polym10050487.

(37) Feng, G.; Li, J.; Colberts, F. J. M.; Li, M.; Zhang, J.; Yang, F.; Jin, Y.; Zhang, F.; Janssen, R. A. J.; Li, C.; et al. " Double-Cable " Conjugated Polymers with Linear Backbone toward High Quantum E Ffi Ciencies in Single-Component Polymer Solar Cells. *J. Am. Chem. Soc.* **2017**, *139*, 18647–18656. https://doi.org/10.1021/jacs.7b10499.

(38) Schill, J.; Milroy, L.-G.; Lugger, J. A. M.; Schenning, A. P. H. J.; Brunsveld, L. Relationship between Side-Chain Polarity and the Self-Assembly Characteristics of Perylene Diimide Derivatives in Aqueous Solution. *ChemistryOpen* **2017**, *6* (2), 266–272. https://doi.org/10.1002/open.201600133.

(39) Kozma, E.; Grisci, G.; Mróz, W.; Catellani, M.; Eckstein-Andicsovà, A.; Pagano, K.; Galeotti, F. Water-Soluble Aminoacid Functionalized Perylene Diimides: The Effect of Aggregation on the Optical Properties in Organic and Aqueous Media. *Dye. Pigment.* **2016**, *125*, 201–209. https://doi.org/10.1016/j.dyepig.2015.10.019.

(40) Shetty, A. S.; Zhang, J.; Moore, J. S. Aromatic π-Stacking in Solution as Revealed through the Aggregation of Phenylacetylene Macrocycles. *J. Am. Chem. Soc.* **1996**, *118* (5), 1019–1027. https://doi.org/10.1021/ja9528893.

(41) Rahman, M. H.; Liao, S.-C.; Chen, H.-L.; Chen, J.-H.; Ivanov, V. A.; Chu, P. P. J.; Chen, S.-A. Aggregation of Conjugated Polymers in Aromatic Solvent. *Langmuir* **2009**, *25* (3), 1667–1674. https://doi.org/10.1021/la802526d.

(42) Shao, C.; Grüne, M.; Stolte, M.; Würthner, F. Perylene Bisimide Dimer Aggregates: Fundamental Insights into Self-Assembly by NMR and UV/Vis Spectroscopy. *Chem. - A Eur. J.* **2012**, *18* (43), 13665–13677. https://doi.org/10.1002/chem.201201661.

(43) Pluczyk, S.; Kuznik, W.; Lapkowski, M.; Reghu, R. R.; Grazulevicius, J. V. Electrochimica Acta The Effect of the Linking Topology on the Electrochemical and Spectroelectrochemical Properties of Carbazolyl Substituted Perylene Bisimides. *Electrochim. Acta* **2014**, *135*, 487–494. https://doi.org/10.1016/j.electacta.2014.05.057.

(44) Li, Q.; Guo, H.; Yang, X.; Zhang, S.; Zhang, H. Synthesis , Characterization , Photophysical Properties and Stability of Bay-Substituted Tetrachloro-Perylene Diimide Dianion Salt by Alkali Treatment. *Tetrahedron* **2017**, *73* (47), 6632–6636. https://doi.org/10.1016/j.tet.2017.10.013.

(45) Yang, J.; Miao, H.; Wei, Y.; Li, W.; Zhu, Y. Π–Π Interaction between Self-Assembled Perylene Diimide and 3D Graphene for Excellent Visible-Light Photocatalytic Activity. *Appl. Catal. B Environ.* **2019**, *240*, 225–233. https://doi.org/10.1016/j.apcatb.2018.09.003.

(46) Angelella, M.; Wang, C.; Tauber, M. J. Resonance Raman Spectra of a Perylene Bis(dicarboximide) Chromophore in Ground and Lowest Triplet States. *J. Phys. Chem. A* **2013**, *117* (38), 9196–9204. https://doi.org/10.1021/jp407879k.

(47) Gora, M.; Krzywiec, W.; Mieczkowski, J.; Rodrigues Maia, E. C.; Louarn, G.; Zagorska, M.; Pron, A. Alternating Copolymers of Diketopyrrolopyrrole or Benzothiadiazole and Alkoxy-Substituted Oligothiophenes: Spectroscopic, Electrochemical and Spectroelectrochemical Investigations. *Electrochim. Acta* **2014**, *144*, 211–220. https://doi.org/10.1016/j.electacta.2014.07.147.

(48) Mombrú, D.; Romero, M.; Faccio, R.; Mombrú, A. W. Raman and Impedance Spectroscopy under Applied Dc Bias Insights on the Electrical Transport for Donor:Acceptor Nanocomposites Based on Poly(vinyl Carbazole) and TiO2 Quantum Dots. *J. Phys. Chem. C* **2017**, *121* (42), 23383–23391. https://doi.org/10.1021/acs.jpcc.7b08400.

(49) Kortekaas, L.; Lancia, F.; Steen, J. D.; Browne, W. R. Reversible Charge Trapping in Bis-Carbazole-Diimide Redox Polymers with Complete Luminescence Quenching Enabling Nondestructive Read-Out by Resonance Raman Spectroscopy. *J. Phys. Chem. C* **2017**, *121* (27), 14688–14702. https://doi.org/10.1021/acs.jpcc.7b04288.

(50) Zhao, L.; Wagner, P.; Elliott, A. B. S.; Griffith, M. J.; Clarke, T. M.; Gordon, K. C.; Mori, S.; Mozer, A. J. Enhanced Performance of Dye-Sensitized Solar Cells Using Carbazole-Substituted Di-Chromophoric Porphyrin Dyes. *J. Mater. Chem. A* **2014**, *2* (40), 16963–16977. https://doi.org/10.1039/c4ta03226h.

(51) Miyoshi, N.; Tomita, G. Production and Reaction of Singlet Oxygen in Aqueous Micellar Solutions Using Pyrene as Photosensitizer. *A J. Chem. Sci.* **1978**, *33* (6), 622–627. https://doi.org/https://doi.org/10.1515/znb-1978-0612.

(52) Wainwright, M.; Grice, N. J.; Pye, L. E. C. Phenothiazine Photosensitizers: Part 2. 3,7-Bis(arylamino)phenothiazines1See Ref.[1].1. *Dye. Pigment.* **1999**, *42* (1), 45–51. https://doi.org/10.1016/S0143-7208(99)00008-X.

(53) Howard, J. A.; Mendenhall, D. G. Autoxidation and Photooxidation of 1,3-Diphenylisobenzofuran: A Kinetic and Product Study. *Can. J. Chem.* **1975**, *53* (14), 2199–2201.

(54) Cai, J.; Huang, J.; Yu, H.; Ji, L. Synthesis, Characterization, and Photocatalytic Activity of TiO2 Microspheres Functionalized with Porphyrin. *Int. J. Photoenergy* **2012**, *2012*, 1–10. https://doi.org/10.1155/2012/348292.

(55) Tobin, J.; Liu, J.; Hayes, H.; Demleitner, M.; Ellis, D.; Arrighi, V.; Xu, Z.; Vilela, F.

BODIPY-Based Conjugated Microporous Polymers as Reusable Heterogeneous Photosensitisers in a Photochemical Flow Reactor. *Polym. Chem.* **2016**, *7* (43), 6662–6670. https://doi.org/10.1039/C6PY01393G.